Title: The 2,6-diaminopurine as a highly potent corrector of UGA nonsense mutations in cancers and other genetic diseases

Authors: Carole Trzaska[1†], Séverine Amand[2†], Christine Bailly[2†], Catherine Leroy[1], Virginie Marchand[3], Evelyne Duvernois-Berthet[4], Jean-Michel Saliou[5], Hana Benhabiles[1], Elisabeth Werkmeister[6], Thierry Chassat[7], Romain Guilbert[7], David Hannebique[7], Anthony Mouray[7], Marie-Christine Copin[1], Pierre-Arthur Moreau[8], Anne Prévotat[9], Philippe Reix[10], Dominique Hubert[11], Michèle Gérardin[12], Eric Adriaenssens[13], Andreas Kulozik[14], Eric Westhof[15], David Tulasne[1], Yuri Motorin[16], Sylvie Rebuffat[2] and Fabrice Lejeune[1,*]

Affiliations:
[1] Univ. Lille, CNRS, Institut Pasteur de Lille, UMR 8161 - M3T – Mechanisms of Tumorigenesis and Target Therapies, F-59000 Lille, France.

[2]Muséum national d'Histoire naturelle, Centre national de la Recherche scientifique, Laboratory Molecules of Communication and Adaptation of Microorganisms (MCAM), UMR 7245 CNRS-MNHN, CP 54, 57 rue Cuvier, 75005 Paris, France.

[3]Next-Generation Sequencing Core Facility, UMS2008 IBSLor CNRS-Université de Lorraine-INSERM, BioPôle, 9 avenue de la Forêt de Haye, 54505 Vandoeuvre-les-Nancy, France.

[4]Muséum national d'Histoire naturelle, Sorbonne Universités, Centre national de la recherche scientifique, Laboratoire Physiologie moléculaire et adaptations (PhyMA), UMR7221 CNRS-MNHN, CP 32, 57 rue Cuvier, 75005 Paris, France.

[5]CNRS, INSERM, CHU Lille, Institut Pasteur de Lille, U1019, UMR 8204, CIIL‑Centre d'Infection et d'Immunité de Lille, University of Lille, 59000 Lille, France.

[6]BioImaging Center Lille Nord de France, France.

[7]Institut Pasteur de Lille – PLEHTA (Plateforme d'expérimentation et de Haute Technologie Animale), 59019 Lille, France.

[8]Univ. Lille, CHRU Lille, Institut Pasteur de Lille, EA 4483 – IMPECS, UFR Pharmacie, F-59000 Lille.

[9] Univ. Lille, Clinique des Maladies Respiratoires, CRCM Hôpital Calmette, CHRU Lille, France.

[10] CRCM pédiatrique Lyon. Hôpital Femme Mère Enfant. Hospices Civils de Lyon. UMR 5558 (EMET). CNRS, LBBE, Université de Lyon, Villeurbanne France.

[11] Pulmonary Department and Adult CF Centre, Cochin Hospital, AP-HP, Paris, France.

[12] CF pediatric centre, Robert Debré hospital, AP-HP, Paris, France.

[13] INSERM U908, Cell plasticity and Cancer, University of Lille 59655 Villeneuve d'Ascq.

[14] Department of Pediatric Oncology, Hematology and Immunology, Children's Hospital and Hopp Children's Tumor Center Heidelberg, EMBL/Medical Faculty Molecular Medicine Partnership Unit Im Neuenheimer Feld 430, D-69120 Heidelberg, Germany.

[15]Architecture and Reactivity of RNA, Institute of Molecular and Cellular Biology of the CNRS UPR9002/University of Strasbourg, Strasbourg, 67084, France.

[16] Ingénierie Moléculaire et Physiopathologie Articulaire, UMR7365, CNRS - Université de Lorraine, 9 avenue de la Forêt de Haye, 54505 Vandoeuvre-les-Nancy, France.

[†] equally contributed to the work

* To whom correspondence should be addressed. Tel: 33 320871059; Fax: 33 320871111; Email: fabrice.lejeune@inserm.fr

One Sentence Summary: 2,6-diaminopurine is an exclusive and efficient UGA readthrough activator.

Abstract:

Nonsense mutations cause about ten percent of genetic disease cases, and no treatments are available for these patients. Nonsense mutations can be corrected by molecules with nonsense mutation readthrough activity. Recently, an extract of the mushroom *Lepista inversa* has shown high-efficiency correction of UGA and UAA nonsense mutations. One active constituent of this extract is 2,6-diaminopurine (DAP). With high efficiency, DAP exclusively corrects UGA nonsense mutations in various cell lines, *in vivo* in mouse models, and in patient cells. The mechanism of action of DAP is through interference with the activity of a tRNA-specific 2'-O-methyltransferase (FTSJ1) that is responsible for Cm34 formation in tRNA[Trp]. Low toxicity and high-efficiency UGA nonsense mutation correction make DAP a good candidate for the development of treatments for genetic diseases caused by nonsense mutations.

Introduction

Nonsense mutations cause about 10% of genetic disease cases [1]. The presence of a premature termination codon (PTC) on an mRNA often activates the mRNA surveillance mechanism called nonsense-mediated mRNA decay (NMD), involving the main NMD factors UPF1, UPF2, and UPF3X (also called UPF3b) [2,3,4,5,6]. NMD specifically degrades PTC-containing mRNAs, thus preventing the synthesis of potentially harmful or nonfunctional truncated proteins. However, a fraction of PTC-containing mRNAs escape from NMD leaving open the possibility to act on them to correct nonsense mutations [7]. As to date no treatments are available for patients with a genetic disease caused by a nonsense mutation. The identification of efficient nonsense mutation correctors is a major public health issue.

At the translational level, PTC recognition is closely related to the mechanism of termination. When the ribosome reaches a stop codon, competition occurs at the A site of the ribosome

between near-cognate tRNAs and the release factors eRF1 and eRF3 in eukaryotes. The result of this competition is 99.9% release factor recruitment, making translation a high-fidelity process during gene expression [8]. To ensure codon translation by cognate tRNAs, these are subject to various posttranscriptional modifications (including methylation, pseudouridylation, deamination and diverse complex modifications especially at positions 34 and 37 of the anticodon) with consequences for genome decoding [9,10,11]. tRNA anticodon modifications, including 2'-O-methylations, play a major role in efficient, error-free decoding of mRNA codons. Many enzymes involved in tRNA modifications have been clearly linked to human pathologies and diseases [12,13].

PTC readthrough during translation involves incorporation, by the ribosome, of an amino acid at the PTC position, so as to complete synthesis of the peptide chain encoded by the open reading frame [14,15,16,17]. A full-length protein synthesized by PTC readthrough results in a difference of no more than one amino acid between the protein synthesized and the wild-type protein. The protein is functional if the amino acid incorporated at the PTC position is compatible with the function of the protein. Recently, PTC readthrough has been shown to occur in specific cytoplasmic bodies called readthrough-bodies, suggesting that a specific environment may favor PTC-readthrough [18].

Strategies aiming to correct nonsense mutations and rescue expression of PTC-containing genes include inhibition of NMD, associated or not with activation of PTC readthrough [14,15,18,19,20]. Several molecules have been shown to activate readthrough, including members of the aminoglycoside family, such as gentamicin and G418, and non-aminoglycosides, such as PTC124/ataluren/Translarna and RTC13/14 [21,22,23,24,25,26,27,28,29]. Some of the compounds used, such as G418 and amlexanox, can both inhibit NMD and activate readthrough

[19,30]. Unfortunately, most of these molecules are either toxic or promote only low-efficiency correction of nonsense mutations in human cells. To date, only PTC124/ataluren/Translarna has reached clinical phase II/III, for cystic fibrosis and Duchenne muscular dystrophy. As the results, albeit encouraging, were too limited to offer patients a significant benefit, the development of this molecule was terminated, at least for these two pathologies [31,32].

In a recent report, we describe a specific screening system for identifying compounds that efficiently correct nonsense mutations in human cells. It uses a firefly reporter gene carrying a nonsense mutation and an intron located more than 55 nucleotides downstream, making the corresponding mRNA subject to NMD [33]. This system, unlike other, previously described screening systems using PTC-containing reporter mRNAs immune to NMD, reproduces the fate of PTC-containing mRNAs in patient cells [21,33,34,35]. We have used it to show that an extract of the common mushroom *Lepista inversa* (H7) acts as a very efficient corrector of UGA and UAA nonsense mutations in human cells [33].

In the present study we have identified the active compounds responsible for the readthrough activity of H7 extract, one of them being 2,6-diaminopurine (DAP). DAP has been previously used for antileukemia treatment and has been injected into children without showing any signs of toxicity [36]. Other activities have been reported for DAP, such as antiviral activity [37,38,39] and inhibition of miRNA activity [40]. DAP is shown here to be an efficient and exclusive corrector of UGA nonsense mutations in immortalized human cells, in patient cells, and *in vivo* in a mouse model. At the molecular level, DAP inhibits Cm_{34} methylation of $tRNA^{Trp}$ by tRNA:methyltransferase 1 (FTSJ1), the human homolog of yeast TRM7, which also catalyzes formation of Cm_{32} and Nm_{34} in some tRNAs, such as $tRNA^{Phe}$ and $tRNA^{Trp}$ [41,42].

Materials and Methods

Cell culture and treatment

HeLa cells were grown in DMEM (Gibco) supplemented with 10% serum (Gibco) and 1% Zellshield. The cell lines Calu-6 and HCC827-GR6 (a generous gift from Pr. P.A. Jänne, Dana-Farber Cancer Institute, Boston, MA, U.S.A.) [43] were grown in RPMI 1640 (Gibco) supplemented with 10% serum (Gibco) and 1% Zellshield. Cystic fibrosis patient cells were grown in BESM medium (Lonza Biosciences).

Cell transfections were performed with lipofectamine 3000 (Life technologies) according to the supplier's recommendations.

Constructs

Fluc-int-UGA has been described in [33]. Expression vectors for FTSJ1/TRM7 (pEZ-V1624-M68-FTSJ1) and CTU1 (pEX-H4779-M02) were purchased from GeneCopoeia (Rockville, USA).

Fractionation of Lepista inversa *extract H7*

As previously described in Benhabiles et al. (2017), H7 extract was obtained from freeze-dried *L. inversa* mushrooms. These were crushed in a mortar and subjected to three successive extractions with methanol/water 50:50 v:v. Concentrating the H7 extract under reduced pressure (Rotavapor, Büchi) yielded fraction F87-1. Fraction F87-1 was solubilized in water and partitioned with organic solvents of increasing polarity (cyclohexane, methylene chloride, ethyl acetate, and butanol successively), yielding five fractions (F87-2 to F87-5). The residual aqueous phase was named F87-6 (Figure 1A). Fraction F87-5, a butanol phase of F87-1, was fractionated by semi-preparative HPLC on a C18 Eclipse XDB column (21.2 x 150 mm, 5 µm;

Agilent Technologies) coupled to a Diode Array Detector (Agilent Technologies 1260 Infinity instrument). The mobile phases were (A): 95% water (0.05% trifluoroacetic acid), 5% acetonitrile and (B): 5% water (0.05% TFA), 95% acetonitrile. Separation was carried out at a flow rate of 10 mL/min, with the following gradient: 100% A for 6 min, 100 to 50% A in 30 min, 50 to 0% A in 2 min, 100% B for 2 min, 0 to 100% A in 2 min, and 100% A for 2 min. Compounds were detected at 210 nm and 254 nm. Nine fractions, numbered F7 to F15, were obtained (Figure 1A). From 40 mg of fraction F87-5, respectively 1.4 mg, 2.4 mg, and 1.6 mg of fractions F10 (Rt at 5.0 min), F13 (Rt at 7.0 min), and F15 (Rt at 9.5 min) were recovered. All organic solvents and reagents (acetonitrile, trifluoroacetic acid) were of HPLC grade purity (Ref. 83639.320 and Ref. 153112E, VWR, France). Ultrapure water obtained with a MilliQ water system (Millipore) was used for HPLC.

Structure analysis by NMR and mass spectrometry

NMR spectra were recorded at 298K on either a 400 MHz Bruker Avance III HD or a 600 MHz Avance II spectrometer (Bruker Biospin). Clitocine and DAP samples were dissolved in D_2O (Eurisotop, France) and placed in 5-mm Wilmad tubes (Eurisotop, France). ^1H and ^{13}C resonance assignments were carried out by means of a series of 1D ^1H and ^{13}C spectra and 2D ^1H COSY, and ^1H-^{13}C HSQC and HMBC experiments.

ESI mass spectra were recorded with a hybrid ESI-Qq-TOF instrument (API Q-Star Pulsar I; Applied Biosystems-Thermo Fisher Scientific) operating in the positive ion detection mode. NMR and mass spectra were analyzed and compared with those obtained with authentic samples of clitocine (Ref. A-7052, Azur Isotopes, France) and DAP (Ref. 247847, Sigma, France).

Preparation of S9 mix

The S9 mix was composed of 5 mM glucose-6-phosphate (Ref. G7879, Batch No.SLBP253V, Sigma, France), 33.5 mM KCl (Ref. P3911, Batch No. SLBQ3328V, Sigma, France), 8 mM MgCl$_2$ (Ref. M8266, Batch No. SLBK9099V, Sigma, France), 4 mM β-NADP (Ref. N5755, Batch No. SLBJ7935V, Sigma, France), and 100 mM NaH$_2$PO$_4$ (Ref. S3139, Batch No. BCBT3558, Sigma, France) in ultrapure water (Ref. BE51200, Batch No. BCBT3558, Lonza, France). Seventy-five microliters (75 µl) of human liver S9 fraction (Pooled Human Liver S9, 20 mg/ml, Ref. 452961, BD, France) was then added to 1380 µl of this S9 mix. The solution was warmed for 15 minutes at 37°C in a thermostatted water bath. The final protein concentration was 1 mg/ml after addition of working solutions.

Protein extraction

Proteins were extracted from $2x10^6$ cells in lysis buffer containing 5% SDS, 50 mM Tris-HCl pH 7, 20 mM EDTA, and a protease inhibitor cocktail (HALT Protease Inhibitor Cocktail, Pierce-Biotechnology, Rockford, IL, USA). Lysates were subjected to 30 pulses of sonication (Branson Digital Sonifier/amplitude 20%) before a 5-min centrifugation at 8000g.

Western blotting

The equivalent of $2.5x10^5$ cells was subjected to 10% SDS-PAGE before transfer of the proteins to a nitrocellulose membrane. The membranes were incubated overnight at 4°C in the presence of a 1/200 dilution of anti-p53 antibody (DO1) (Santa Cruz Biotechnology, Dallas, TX, USA), or a 1/1000 dilution of anti-CBP80 (H-300) antibody (Santa Cruz Biotechnology, Dallas, TX, USA). After three washes of the membrane in TBS Tween, the membranes were exposed to a

solution of peroxidase-coupled secondary antibody for detection of mouse- or rabbit-raised antibody (Jackson ImmunoResearch, Suffolk, UK). Antibodies were then detected with Super Signal West Femto Maximum Sensitivity Substrate (Pierce-Biotechnology, Rockford, IL, USA). Quantifications were performed with QuantityOne software (Biorad).

RT-PCR

The RT-PCR procedure and the primers used in this study have been described previously [19].

Firefly luciferase assay

Firefly luciferase assay was performed as described previously [33].

Micronucleus induction assay

The assay was performed by CytoxLab (Evreux, France). Briefly, L5178 TK$^{+/-}$ mouse cells were exposed to three concentrations of DAP for 24 or 3 h, followed by a 24-h recovery period when the experiment was performed in the presence of Aroclor-induced rat liver S9 metabolizing mix (at 2% final concentration). As positive control, mitomycin C was used at 1 µg/ml in experiments without S9 mix and cyclophosphamide at 6 µg/ml in experiments with S9 mix. The nuclei were then stained with Giemsa before counting the micronuclei among 1000 mononucleated cells.

Treatment of cystic fibrosis patient cells to measure CFTR function

Cell growth and treatment conditions have been described previously [33]. All cystic fibrosis patient cells used in this study were obtained under authorization of the local ethics committee

"Comité de Protection des Personnes Nord Ouest IV". Patients were informed about the study and provided written consent.

Toxicity assay

The toxicity assay was performed 24 h after starting cell treatment. Cell culture supernatant was centrifuged at 6000g for 10 min to pellet cells and cell debris. One-twentieth of the supernatant was then used to measure adenylate kinase activity according to the supplier's protocol (Lonza Biosciences, Basel, Switzerland).

In vivo assay

To initiate tumor growth, six-week-old nude mice received subcutaneously 10 million cells suspended in PBS. Starting 24 h after injection, the mice were force-fed daily with 200 µl DMSO or DAP solution at 5mg/ml. Tumors were measured three times weekly for three weeks to determine the tumor volume by the following formula: l (mm)xL (mm)xL (mm). The tumors were then collected and a fraction was used for western blot analysis after protein extraction.

tRNA modification analysis

tRNAs were purified with RNAzol (MRC, Cincinnati, OH, USA) from HeLa cells exposed for 24 h to DMSO or 25 µM DAP, according to the manufacturer's protocol. The detailed protocol and a description of the RiboMethSeq assay are provided elsewhere [44].

DAP affinity columns

Two hundred milligrams of Epoxy-activated Sepharose 6B (GE Healthcare) was suspended in distilled water and washed with 80 ml distilled water and then divided into two samples. Coupling was performed by adding 100 µmol of DAP suspended in 10 N NaOH to the first sample and incubating for 16 h at 37°C under gentle stirring. The packing for the "empty column" was obtained by adding 1 ml of 10 N NaOH to the second sample and proceeding similarly. The columns were then washed with 10 N NaOH and the remaining active groups were blocked by incubating the columns with ethanolamine at pH 8 overnight at 37°C. The columns were further washed with three cycles of 0.1 M CH_3COOK pH 4 containing 0.5 M NaCl, followed by 0.1 M Tris-HCl pH 8 containing 0.5 M NaCl. Each column was then incubated overnight at 4°C under gentle stirring with an amount of extract equivalent to 120 million cells, in the presence of HALT Protease Inhibitor Cocktail (Pierce). The columns were then washed five times with a buffer containing 50 mM Tris-HCl pH 7.4, 300 mM NaCl, and 0.05% NP40, before elution with 100 µl of 100 mM DAP dissolved in DMSO.

Amino-acid identification assay

Sixty million HEK293FT cells were transfected with 120 µg Fluc-int-UGA construct with $CaCl_2$ in HBSS buffer. After a 24-h incubation at 37°C under 5% CO_2, the cells were exposed for 24 h to 25 µM DAP or to DMSO as negative control, before immunoprecipitation of firefly luciferase with anti-firefly luciferase antibody (EDM Millipore, Temecula, USA) according to the protocol described in [45]. The immunoprecipitate was subjected to 10% SDS-PAGE and then firefly luciferase was detected by Coomassie staining. The band at 64 kDa present in DAP-treated cells but not in cells exposed to DMSO was excised for in-gel digestion with chymotrypsin. NanoLC-

MSMS analysis of the protein digest was performed on a UltiMate-3000 RSLCnano System coupled to a Q-Exactive instrument (Thermo Fisher Scientific).

MS/MS data were interpreted with the Mascot search engine (version 2.4.0, Matrix Science, London, UK) installed on a local server. Searches were performed with a tolerance on mass measurement of 10 ppm for precursor ions and 0.02 Da for fragment ions, against a database built with Fluc sequences degenerated at Tyr109, recombinant trypsin, and a list of classical contaminants (138 entries). Cysteine carbamidomethylation, methionine oxidation, protein N-terminal acetylation, and cysteine propionamidation were searched as variable modifications. Up to three missed chymotrypsin cleavages were allowed.

DAP stability assay

The assay was performed by C-Ris Pharma, Saint Malo, France. Briefly, DAP at 10 mM was diluted in S9 mix (to 300 µM final concentration) and acetonitrile extraction was performed either immediately (T0) or after a 4-h incubation at 37°C. The samples were then centrifuged and directly analyzed by LC-MS. The extraction efficiency was estimated at 97.2%. After extraction, the collected supernatants were directly injected into the HPLC for analysis. Analysis was performed by MS to allow detection of potential metabolite(s).

Results

DAP contributes to the nonsense-mutation-correcting activity of Lepista inversa *extract.*

An extract (H7) prepared from the mushroom *Lepista inversa* (also called *Paralepista flaccida*) has recently been shown to exhibit high UAA and UGA readthrough activity [33]. To identify the compounds responsible for this activity, a semi-preparative High Performance Liquid

Chromatography (HPLC) fractionation protocol was used. Nine fractions (F7 to F15) were obtained (Fig. 1A) and tested for PTC-readthrough activity in a system using firefly luciferase mRNA carrying a PTC and subject to NMD (Fig. 1B and [33]). DMSO and G418 were used, as a negative and a positive control, respectively. As expected [33], G418 corrected the UGA more efficiently than the UAG nonsense mutation and only weakly corrected the UAA nonsense mutation. Firefly luciferase activity measurements showed that fractions F13 and F15 correct the UAA nonsense mutation while fractions F10, F13, and F15 correct the UGA nonsense mutation (Fig. 1C). The combined use of nuclear magnetic resonance (NMR) and mass spectrometry allowed identifying the major component in fractions F13 and F15 as clitocine ((2R,3R,4S,5R)-2-[(6-amino-5-nitropyrimidin-4-yl)amino]-5-(hydroxymethyl)oxolane-3,4-diol) (76% and 47%, respectively), known as a potent readthrough molecule [24]. In fraction F10 another molecule, present at about 77%, was assigned to 2,6-diaminopurine (DAP) on the basis of the ^{1}H NMR analysis, and mass fragmentation data, and showed exclusive readthrough of the UGA stop codon (Fig. 1C). To demonstrate that the UGA readthrough activity exhibited by fraction F10 was due to DAP and not to another minor compound, commercial DAP (98% purity) was tested for PTC-readthrough activity and showed exclusive correction of the UGA nonsense mutation. This confirms that the readthrough activity of fraction F10 is related to the presence of DAP (Fig. 1C). Given the toxicity issues associated with clitocine [46], we decided to focus on DAP. The half-maximal effective concentration (EC50) of DAP was then determined on the firefly luciferase constructs, with increasing amounts of DAP or G418 (as a reference molecule) in the cell culture medium (Fig. 1D). DAP showed maximal efficacy at 100 µM, with an EC50 at about 50 µM. Notably, at 6.25µM, it was 10 times as effective as 600µM G418, and at 100µM, it reached 200 times as effective as 600µM G418.

DAP corrects endogenous nonsense mutations in various cell lines

To further assess its nonsense-mutation-correcting efficiency, DAP was added to the culture medium of cancer cell lines harboring an endogenous nonsense mutation in the TP53 gene [33]. After 24 hours of treatment, proteins were extracted from the cells and the p53 protein was assessed by western blotting (Fig. 2). As anticipated, p53 protein was not detected after DMSO mock treatment due to the presence of the PTC in p53 mRNA [33]. DAP treatment allowed dose-dependent synthesis of the p53 protein in Calu-6 cells (UGA nonsense mutation), but not in Caco-2 cells (UAG nonsense mutation) or Caov-3 cells (UAA nonsense mutation). This is consistent with the results in Fig. 1C and confirms that DAP exclusively corrects the UGA nonsense mutation. The p53 protein was detected after DAP treatment at concentrations as low as 1.56 µM, while it was barely detected upon treatment with 25 µM G418. This is consistent with the results of Fig. 1C, showing that DAP corrects the UGA nonsense mutation more efficiently than G418.

Even if DAP promotes the synthesis of full-length proteins from UGA-nonsense-mutation-containing mRNAs, it is necessary to ascertain that the readthrough protein is functional. Such evidence was first provided by the high luciferase activity observed after DAP treatment (Fig. 1C, 1D), indicating that the enzyme is functional. Three additional assays were used to further demonstrate that DAP promotes the synthesis of functional full-length proteins from PTC-containing mRNAs. The first assay involved measuring the transcriptional activity of the p53 readthrough protein in Calu-6 cells. Cells were transfected with an expression vector carrying the cDNA encoding firefly luciferase under a promoter with two p53-responsive elements (Fig. 3A) [33]. Upon DMSO treatment, only a basal luciferase activity was detected, reflecting promoter

leakage (Fig. 3B). In the presence of increasing amounts of G418, the luciferase activity remained at the background level, indicating that G418 does not promote synthesis of a functional full-length p53 protein. In contrast, upon DAP treatment, the luciferase activity significantly increased, clearly demonstrating that the p53 readthrough protein synthesized upon DAP treatment in Calu-6 cells is functional. The second assay used a p53 target gene such as p21 [47]. The level of p21 mRNA was monitored by quantitative RT-PCR in Calu-6 cells exposed to DMSO, G418, or DAP (Fig. 3C). It was found to increase significantly in cells exposed to DAP, but not in the presence of G418. This second assay thus confirmed that DAP promotes the synthesis of a functional p53 protein in Calu-6 cells, more efficiently than does G418.

Finally, in a third assay, the functionality of a readthrough protein produced upon DAP treatment was evaluated on cystic fibrosis patient cells homozygotic for a UGA nonsense mutation in the cystic fibrosis transmembrane conductance regulator (CFTR) gene collected from three patients recruited from three French cystic fibrosis reference centers. The cells were incubated with DMSO, G418, or DAP followed by the measurement of the iodine flux through the cell membrane, which reflects the functionality of the CFTR (Fig. 3D) [33,48]. In all three patient cells, DAP promoted the most efficient iodine transport through the cell membrane.

Overall, the results shown in Fig.1 and 3 indicate that in the four tested models, DAP activates readthrough of UGA nonsense mutations to promote synthesis of functional readthrough proteins.

DAP does not inhibit NMD

Correction of UGA nonsense mutations by DAP might result from combined effect of NMD inhibition and readthrough activity, as shown for other molecules [19,30], or from readthrough

activation only. To check if DAP inhibits NMD, the efficiency of NMD was monitored by measuring the level of p53 mRNA in the presence of DMSO, DAP, or G418 (Fig. 4A). Total RNA was purified from Calu-6 cells after 24 hours treatment. At both tested concentrations, DAP failed to significantly inhibit NMD, unlike G418, which showed 1.8 time fold increase in p53 mRNA. This is consistent with previous reports demonstrating that G418 can both inhibit NMD and activate readthrough [19,30]. The fact that DAP does not affect NMD is also consistent with the observation that no inhibition of NMD was previously detected upon treatment with the H7 extract [33].

DAP shows low toxicity

Although DAP-containing H7 extract does not appear to be toxic [33], the toxicity of DAP was assessed by measuring the adenylate kinase activity in the culture medium of HeLa cells treated with DMSO, DAP, or the apoptosis inducer staurosporine (STS) used as a positive control (Fig. 4B). After 24 hours of treatment, the release of adenylate kinase activity was detected for the cells exposed to STS, but not for the cells exposed to increasing amounts of DAP. This indicates that DAP is not cytotoxic, at least under these experimental conditions. This conclusion was supported by a second toxicity assessment focusing on the putative impact of DAP on DNA integrity. Briefly, mouse L5178Y TK$^{+/-}$ cells were exposed to DMSO or DAP for 24 hours or 3 hours followed by 24 hours recovery, in the absence or presence of Aroclor-induced rat liver S9 fraction, so as to reproduce the metabolizing conditions prevailing in the liver. Cells with nucleus injury, and particularly those with small nuclei, were then counted, these features being indicative of DNA damage and hence of tested-compound genotoxicity (Table 1). No significant

increase in the number of micronucleated cells was measured. Overall, these results demonstrate that DAP is not genotoxic.

To complete the study on the putative DAP toxicity, we evaluated the consequences of DAP treatment on gene expression at the transcription and at the translation levels. First, in HeLa cells, we assessed the impact of DAP on the whole transcription profile, as compared with the treatment by DMSO. No more than 0.13% of the genes (i.e. 30 genes out of 22935 human genes analyzed) showed more than 4-fold up- or downregulation (adjusted p-value <0.05, |log2FC|>= 2). More importantly, no pathway was found to be specifically upregulated by DAP (Table 2 and Fig. S1). This analysis suggested that DAP does not target any specific metabolic pathway and that the 0.13% gene variation measured could be a nonspecific response to an unusual component in the cell. Secondly, 2D differential gel electrophoresis (2D-DIGE) was performed on the whole proteomes of HeLa cells exposed to DMSO or DAP. No visible differences were observed between the two proteomes (Fig. S2). Altogether, these results unambiguously indicate that DAP does not interfere at the mRNA or protein level with the gene expression program of HeLa cells strengthening the absence of toxicity in human cells observed at the Fig. 4B.

DAP corrects nonsense mutations in vivo

Stability of DAP under simulated *in vivo* conditions was assessed in human liver S9 extract to mimic the liver environment [49]. After 4 hours incubation, DAP and its metabolites were extracted by acetonitrile and subjected to HPLC/mass spectrometry analysis. No DAP-derived metabolites were detected under these experimental conditions, and recovery of the molecule after incubation exceeded 80%, indicating that DAP is stable and suggesting that it should be stable *in vivo* as well, since the liver is the main site of drug degradation in the body (Fig. 5A).

Next, the *in vivo* capacity of DAP to correct UGA nonsense mutations was assessed in a mouse model. Four-week-old immunodeficient nude mice were injected with identical number of Calu-6 cells carrying a UGA nonsense mutation in the TP53 gene or HCC-GR6 cells having a wild-type TP53 gene but carrying different tumor-inducing mutations (a small deletion in the EGFR gene and an amplification of MET gene leading to the constitutive activation of both receptors) [43]. For three weeks, the mice were forced-fed every day with DMSO or DAP and tumor growth was monitored three times per week. We assumed that if DAP induces expression of a functional p53 protein in Calu-6 cells, these cells should divide more slowly and enter apoptosis as previously reported [24]. After three weeks of treatment, a significant difference was observed between Calu-6-cell-injected mice exposed to DMSO and ones exposed to DAP (Fig. 5B – left panel): DAP strongly impaired tumor growth as compared to DMSO. In contrast, when HCC-GR6 cells were used to induce tumor formation, no significant difference in tumor growth between DAP- and DMSO-exposed mice was observed (Fig. 5B – right panel). This suggested that the slow-down tumor growth observed with Calu-6 cells is likely due to rescue of p53 protein synthesis in these cells. Rescue of p53 synthesis was indeed found to occur in the tumors of DAP-treated mice, as assessed by western-blotting (Fig. 5C).

Altogether, these results demonstrated that orally administered DAP rescues functional expression of genes carrying a UGA nonsense mutation *in vivo*.

Molecular mechanism of DAP-driven UGA readthrough

To elucidate the molecular mechanism underlying the DAP-promoted UGA readthrough, mass spectrometry was used to identify the amino acid incorporated at the PTC position into firefly luciferase synthesized from the Fluc-int-UGA construct. HEK293FT cells treated with 25µM

DAP were chosen for their high rate of transfection, crucial to generating enough readthrough protein to be analyzed by mass spectrometry. The luciferase protein was digested with chymotrypsin to generate a PTC-position-containing peptide compatible with mass spectrometry analysis. Using this approach, we found only one amino acid, tryptophan, incorporated at the PTC position in the peptide of interest (Fig. 6A). These results clearly demonstrated that DAP-promoted UGA readthrough is mediated by tRNA^{Trp}, by non-Watson-Crick base-pairing A*C at the Wobble position. Human tRNA^{Trp} was shown to have suppressor functions [50], and plant tRNA^{Trp} (CmCA) was also known to promote UGA readthrough [51].

To ensure accurate recognition, tRNA is subject to numerous posttranscriptional nucleotide modifications, notably in the anticodon triplet at the wobble position N_{34}. Among the enzymes modifying tRNAs liable to recognize a stop codon by extended wobbling, human FTSJ1 (TRM7 in yeast) exclusively modifies tRNAs involved in UGA readthrough [12]. In addition to other tRNA targets, FTSJ1 methylates the cytosine at position 34 of tRNA^{Trp}. Inhibition of this modification increases the capacity of tRNA^{Trp} to recognize the UGA stop codon. To test the hypothesis that DAP interferes with the activity of FTSJ1, HeLa cells were co-transfected with the pFluc-int-UGA construct and with increasing amounts of an expression vector for either FTSJ1 or CTU1 (an uridine thiolase targeting U34 in tRNA^{Gln} and tRNA^{Lys}, probably affecting the recognition of UAA stop codon [52]). The transfected cells were then treated with increasing amounts of DAP (Fig. 6B). Overexpression of FTSJ1, but not of CTUI, was found to strongly reduce DAP-promoted readthrough. This suggests that DAP promotes UGA readthrough by targeting FTSJ1 activity.

To confirm that DAP indeed inhibits FTSJ1 activity, RiboMethSeq analysis was performed to detect modulation of tRNA 2'-O-methylations in the presence of DAP (Fig. 6B and S3). HeLa cells were incubated with DMSO or DAP before extraction of small RNAs, which include tRNAs. RiboMethSeq analysis of human tRNAs was then performed [44]. In the presence of DAP, the level of 2'-O-methylation was significantly lower for three tRNAs, including 2'-O-methylation of tRNA^{Trp} at position 34 (Fig. 6C), while other known Nm positions were not affected (Fig. S3). Although the human targets of FTSJ1 remain poorly characterized, modification of Cm_{34} in tRNA^{Trp} has been attributed to FTSJ1 [41]. It is noteworthy that the second affected tRNA (tRNA^{Gln}) also showed reduced Cm_{32} methylation. This is consistent with DAP-dependent inhibition of FTSJ1 activity. The third hit was 2'-O-methylation of tRNA^{Ser} at position Gm_{18}, attributed to TARBP1 activity. Overall, the results of the RiboMethSeq assay and of FTSJ1 overexpression converge to suggest that DAP acts by inhibiting the action of FTSJ1 at certain 2'-O-methylation sites in human tRNAs.

Whether DAP interacts with FTSJ1 was then investigated by DAP affinity chromatography. The column packing was produced by covalent attachment of DAP to activated epoxy Sepharose beads. The column was then exposed to HeLa cell extract followed by competitive elution of the bound proteins with excess of DAP. The eluate was analyzed by western blotting for the presence of various proteins, including FTSJ1. Out of all tested targets, FTSJ1 was the only protein to be specifically bound to the DAP affinity column and absent in eluate from a column packed with beads alone. These results indicate that DAP binds to FTSJ1 (Fig. 6D).

Discussion

Nonsense mutations cause about ten percent of genetic diseases [1] through silencing of the mutant gene. To date, we lack highly efficient molecules capable of rescuing the expression of genes harboring a nonsense mutation. Here we have focused our study on H7 extract from the common mushroom *Lepista inversa*, recently shown to promote expression of genes carrying UGA or UAA nonsense mutations [33]. Two molecules responsible for the activity of H7 extract were identified, one of those is clitocine, previously shown to correct nonsense mutations more efficiently than G418 [24]. The mode of action of clitocine differs from that of other readthrough activator molecules such as aminoglycosides, shown to interact with the ribosome [53]. Clitocine is incorporated into the mRNA, where it replaces the adenosine base and facilitates stop codon recognition by some near-cognate tRNAs [24]. The second nonsense-mutation-correcting molecule found here in H7 extract is DAP. DAP corrects UGA nonsense mutations only; it is the first molecule showing correction of only one stop codon. The UGA stop codon is the most frequent termination codon, both physiological and premature [54]. Here, in four different assays, we show that DAP promotes the synthesis of functional proteins. DAP also corrects UGA nonsense mutations more efficiently than G418, even though it does not inhibit NMD. Some other molecules such as PTC124/ataluren/Translarna [21], like H7 extract [33], have been shown to promote PTC readthrough without affecting NMD. Remarkably, DAP does not appear to be toxic even at high concentrations. Lastly, it rescues the expression of genes carrying UGA nonsense mutations *in vivo* and can be orally administered.

DAP mode of action appears original, since this molecule targets an enzyme responsible for the posttranscriptional modification of tRNAs. DAP inhibits the activity of FTSJ1 methyltransferase, thus reducing Cm34-methylation in the tRNA^Trp anticodon loop, and, in turn, increasing readthrough at UGA stop codons only. tRNA modifications play essential roles in the fidelity of

codon recognition, and their absence leads to either inefficient translation or to miscoding through binding of near-cognate tRNA. The amino acid inserted at the UGA stop codon is exclusively tryptophan in our experiments, indicating that the near-cognate tRNA^{Trp} is responsible for the read-through and miscodes by forming a $C_{34}oA_{(+3)}$ at the third position of the codon (Trp is in the same codon box than the UGA stop). It is known that tRNA^{Trp} is 2'-O-methylated at position 34 by FTSJ1. Although there is not yet structural evidence, all the evidence points to a stabilization of a Watson-Crick pair at the third position mediated by the methylation leading to a $C_{m34}=G_{(+3)}$ Watson-Crick in the cognate complex). Consequently, the absence of methylation promotes recognition of the UGA stop codon by the near-cognate tRNA^{Trp} [55]. The enzymes responsible for tRNA modifications thus constitute a new set of putative targets for nonsense mutation correction, since their targeted inhibition should promote PTC-readthrough. In addition, as posttranscriptional tRNA modifiers show specificity for particular tRNAs, positions, and modifications, their targeting might be adjusted to allow precise correction of nonsense mutations.

DAP is likely one of the most efficient UGA readthrough activators identified to date. Given its high efficacy and low toxicity, it seems more compatible with a therapeutic approach than previously reported molecules. Another advantage of DAP is its selectivity for the UGA stop codon, which should reduce the risk of potential side effects.

Correctors of nonsense mutations constitute possible drug candidates for the treatment of genetic diseases caused by nonsense mutations. They may also find a place in personalized medicine, since they would be used for patients with a particular mutation rather than for all patients with the same pathology. Only a fraction of patients suffering from a wide range of diseases should benefit from stimulated readthrough therapy. The readthrough molecules identified so far are

either highly toxic (e.g. aminoglycosides and clitocine) or not effective enough to offer sufficient therapeutic benefits (e.g. ataluren) [32,56,57,58]. New molecules are being developed in order to address all these issues, such as a derivative of ataluren named PTC414, which has higher efficacy than ataluren [59], and new-generation aminoglycosides [25,60,61], designed to increase the efficiency of readthrough correction and decrease the long-term toxicity associated with the previous generation of aminoglycosides. One of these, named ELX-02, is currently being tested a phase 1B clinical trial for cystic fibrosis (http://www.eloxxpharma.com/pipeline/).

In conclusion, several lines of evidence show that DAP is an excellent drug candidate for the treatment of genetic diseases caused by UGA nonsense mutations. Its correction efficiency is ten to two hundred times that of G418, suggesting that it could have therapeutic benefits. The results obtained on cystic fibrosis patient cells and *in vivo* in a mouse model show that DAP can rescue the function of proteins synthesized from a gene carrying a nonsense mutation. In addition, it has been found to show low toxicity in cell cultures and no detectable toxicity in a mouse model. For all these reasons, DAP may someday offer new hope to patients whose pathology is caused by a UGA nonsense mutation.

References and Notes:

1. Mort M, Ivanov D, Cooper DN, Chuzhanova NA (2008) A meta-analysis of nonsense mutations causing human genetic disease. Hum Mutat 29: 1037-1047.
2. Gupta P, Li YR (2018) Upf proteins: highly conserved factors involved in nonsense mRNA mediated decay. Mol Biol Rep 45: 39-55.
3. Karousis ED, Nasif S, Muhlemann O (2016) Nonsense-mediated mRNA decay: novel mechanistic insights and biological impact. Wiley Interdiscip Rev RNA 7: 661-682.
4. Hug N, Longman D, Caceres JF (2016) Mechanism and regulation of the nonsense-mediated decay pathway. Nucleic Acids Res 44: 1483-1495.
5. Popp MW, Maquat LE (2014) The dharma of nonsense-mediated mRNA decay in mammalian cells. Mol Cells 37: 1-8.

6. Lejeune F (2017) Nonsense-mediated mRNA decay at the crossroads of many cellular pathways. BMB Rep.
7. Kuzmiak HA, Maquat LE (2006) Applying nonsense-mediated mRNA decay research to the clinic: progress and challenges. Trends Mol Med 12: 306-316.
8. Floquet C, Hatin I, Rousset JP, Bidou L (2012) Statistical analysis of readthrough levels for nonsense mutations in mammalian cells reveals a major determinant of response to gentamicin. PLoS Genet 8: e1002608.
9. Han L, Phizicky EM (2018) A rationale for tRNA modification circuits in the anticodon loop. RNA 24: 1277-1284.
10. Tuorto F, Lyko F (2016) Genome recoding by tRNA modifications. Open Biol 6.
11. Grosjean H, Westhof E (2016) An integrated, structure- and energy-based view of the genetic code. Nucleic Acids Res 44: 8020-8040.
12. Guy MP, Shaw M, Weiner CL, Hobson L, Stark Z, et al. (2015) Defects in tRNA Anticodon Loop 2'-O-Methylation Are Implicated in Nonsyndromic X-Linked Intellectual Disability due to Mutations in FTSJ1. Hum Mutat 36: 1176-1187.
13. Sarin LP, Leidel SA (2014) Modify or die?--RNA modification defects in metazoans. RNA Biol 11: 1555-1567.
14. Keeling KM, Xue X, Gunn G, Bedwell DM (2014) Therapeutics based on stop codon readthrough. Annu Rev Genomics Hum Genet 15: 371-394.
15. Benhabiles H, Jia J, Lejeune F (2016) Nonsense mutation correction in human diseases: an approach for targeted medicine; Elsevier, editor: Publisher: Catherine Van Der Laan. 1-192 p.
16. Bidou L, Allamand V, Rousset JP, Namy O (2012) Sense from nonsense: therapies for premature stop codon diseases. Trends Mol Med 18: 679-688.
17. Dabrowski M, Bukowy-Bieryllo Z, Zietkiewicz E (2018) Advances in therapeutic use of a drug-stimulated translational readthrough of premature termination codons. Mol Med 24: 25.
18. Beaudet AL, Meng L (2016) Gene-targeting pharmaceuticals for single-gene disorders. Hum Mol Genet 25: R18-26.
19. Gonzalez-Hilarion S, Beghyn T, Jia J, Debreuck N, Berte G, et al. (2012) Rescue of nonsense mutations by amlexanox in human cells. Orphanet J Rare Dis 7: 58.
20. Linde L, Boelz S, Nissim-Rafinia M, Oren YS, Wilschanski M, et al. (2007) Nonsense-mediated mRNA decay affects nonsense transcript levels and governs response of cystic fibrosis patients to gentamicin. J Clin Invest 117: 683-692.
21. Welch EM, Barton ER, Zhuo J, Tomizawa Y, Friesen WJ, et al. (2007) PTC124 targets genetic disorders caused by nonsense mutations. Nature 447: 87-91.
22. Kayali R, Ku JM, Khitrov G, Jung ME, Prikhodko O, et al. (2012) Read-through compound 13 restores dystrophin expression and improves muscle function in the mdx mouse model for Duchenne muscular dystrophy. Hum Mol Genet 21: 4007-4020.
23. Kuschal C, DiGiovanna JJ, Khan SG, Gatti RA, Kraemer KH (2013) Repair of UV photolesions in xeroderma pigmentosum group C cells induced by translational readthrough of premature termination codons. Proc Natl Acad Sci U S A 110: 19483-19488.
24. Friesen WJ, Trotta CR, Tomizawa Y, Zhuo J, Johnson B, et al. (2017) The nucleoside analog clitocine is a potent and efficacious readthrough agent. RNA.
25. Xue X, Mutyam V, Tang L, Biswas S, Du M, et al. (2014) Synthetic aminoglycosides efficiently suppress cystic fibrosis transmembrane conductance regulator nonsense mutations and are enhanced by ivacaftor. Am J Respir Cell Mol Biol 50: 805-816.
26. Shulman E, Belakhov V, Wei G, Kendall A, Meyron-Holtz EG, et al. (2014) Designer aminoglycosides that selectively inhibit cytoplasmic rather than mitochondrial ribosomes show decreased ototoxicity: a strategy for the treatment of genetic diseases. J Biol Chem 289: 2318-2330.
27. Du L, Damoiseaux R, Nahas S, Gao K, Hu H, et al. (2009) Nonaminoglycoside compounds induce readthrough of nonsense mutations. J Exp Med 206: 2285-2297.
28. Manuvakhova M, Keeling K, Bedwell DM (2000) Aminoglycoside antibiotics mediate context-dependent suppression of termination codons in a mammalian translation system. RNA 6: 1044-1055.
29. Friesen WJ, Johnson B, Sierra J, Zhuo J, Vazirani P, et al. (2018) The minor gentamicin complex component, X2, is a potent premature stop codon readthrough molecule with therapeutic potential. PLoS One 13: e0206158.
30. Correa-Cerro LS, Wassif CA, Waye JS, Krakowiak PA, Cozma D, et al. (2005) DHCR7 nonsense mutations and characterisation of mRNA nonsense mediated decay in Smith-Lemli-Opitz syndrome. J Med Genet 42: 350-357.

31. Kerem E, Hirawat S, Armoni S, Yaakov Y, Shoseyov D, et al. (2008) Effectiveness of PTC124 treatment of cystic fibrosis caused by nonsense mutations: a prospective phase II trial. Lancet 372: 719-727.

32. Kerem E, Konstan MW, De Boeck K, Accurso FJ, Sermet-Gaudelus I, et al. (2014) Ataluren for the treatment of nonsense-mutation cystic fibrosis: a randomised, double-blind, placebo-controlled phase 3 trial. Lancet Respir Med 2: 539-547.

33. Benhabiles H, Gonzalez-Hilarion S, Amand S, Bailly C, Prevotat A, et al. (2017) Optimized approach for the identification of highly efficient correctors of nonsense mutations in human diseases. PLoS One 12: e0187930.

34. Bidou L, Hatin I, Perez N, Allamand V, Panthier JJ, et al. (2004) Premature stop codons involved in muscular dystrophies show a broad spectrum of readthrough efficiencies in response to gentamicin treatment. Gene Ther 11: 619-627.

35. Gurskaya NG, Pereverzev AP, Staroverov DB, Markina NM, Lukyanov KA (2016) Analysis of Nonsense-Mediated mRNA Decay at the Single-Cell Level Using Two Fluorescent Proteins. Methods Enzymol 572: 291-314.

36. Burchenal JH, Karnofsky DA, Kingsley-Pillers EM, Southam CM, Myers WP, et al. (1951) The effects of the folic acid antagonists and 2,6-diaminopurine on neoplastic disease, with special reference to acute leukemia. Cancer 4: 549-569.

37. Friend C (1951) Effect of 2,6-diaminopurine on virus of Russian spring summner encephalitis in tissue culture. Proc Soc Exp Biol Med 78: 150-153.

38. Margolis DM, Mukherjee AL, Fletcher CV, Hogg E, Ogata-Arakaki D, et al. (2007) The use of beta-D-2,6-diaminopurine dioxolane with or without mycophenolate mofetil in drug-resistant HIV infection. AIDS 21: 2025-2032.

39. Zouharova D, Lipenska I, Fojtikova M, Kulich P, Neca J, et al. (2016) Antiviral activities of 2,6-diaminopurine-based acyclic nucleoside phosphonates against herpesviruses: In vitro study results with pseudorabies virus (PrV, SuHV-1). Vet Microbiol 184: 84-93.

40. Kamiya Y, Donoshita Y, Kamimoto H, Murayama K, Ariyoshi J, et al. (2017) Introduction of 2,6-Diaminopurines into Serinol Nucleic Acid Improves Anti-miRNA Performance. Chembiochem 18: 1917-1922.

41. Pintard L, Lecointe F, Bujnicki JM, Bonnerot C, Grosjean H, et al. (2002) Trm7p catalyses the formation of two 2'-O-methylriboses in yeast tRNA anticodon loop. EMBO J 21: 1811-1820.

42. Guy MP, Podyma BM, Preston MA, Shaheen HH, Krivos KL, et al. (2012) Yeast Trm7 interacts with distinct proteins for critical modifications of the tRNAPhe anticodon loop. RNA 18: 1921-1933.

43. Engelman JA, Zejnullahu K, Mitsudomi T, Song Y, Hyland C, et al. (2007) MET amplification leads to gefitinib resistance in lung cancer by activating ERBB3 signaling. Science 316: 1039-1043.

44. Marchand V, Blanloeil-Oillo F, Helm M, Motorin Y (2016) Illumina-based RiboMethSeq approach for mapping of 2'-O-Me residues in RNA. Nucleic Acids Res 44: e135.

45. Lejeune F, Maquat LE (2004) Immunopurification and analysis of protein and RNA components of mRNP in mammalian cells. Methods Mol Biol 257: 115-124.

46. Ren G, Zhao YP, Yang L, Fu CX (2008) Anti-proliferative effect of clitocine from the mushroom Leucopaxillus giganteus on human cervical cancer HeLa cells by inducing apoptosis. Cancer Lett 262: 190-200.

47. el-Deiry WS, Tokino T, Velculescu VE, Levy DB, Parsons R, et al. (1993) WAF1, a potential mediator of p53 tumor suppression. Cell 75: 817-825.

48. Mansoura MK, Biwersi J, Ashlock MA, Verkman AS (1999) Fluorescent chloride indicators to assess the efficacy of CFTR cDNA delivery. Hum Gene Ther 10: 861-875.

49. Duffus JH, Nordberg M, Templeton DM (2007) GLOSSARY OF TERMS USED IN TOXICOLOGY, 2nd EDITION. Pure Appl Chem 79: 1153-1344.

50. Geller AI, Rich A (1980) A UGA termination suppression tRNATrp active in rabbit reticulocytes. Nature 283: 41-46.

51. Urban C, Zerfass K, Fingerhut C, Beier H (1996) UGA suppression by tRNACmCATrp occurs in diverse virus RNAs due to a limited influence of the codon context. Nucleic Acids Res 24: 3424-3430.

52. Dewez M, Bauer F, Dieu M, Raes M, Vandenhaute J, et al. (2008) The conserved Wobble uridine tRNA thiolase Ctu1-Ctu2 is required to maintain genome integrity. Proc Natl Acad Sci U S A 105: 5459-5464.

53. Prokhorova I, Altman RB, Djumagulov M, Shrestha JP, Urzhumtsev A, et al. (2017) Aminoglycoside interactions and impacts on the eukaryotic ribosome. Proc Natl Acad Sci U S A 114: E10899-E10908.

54. Atkinson J, Martin R (1994) Mutations to nonsense codons in human genetic disease: implications for gene therapy by nonsense suppressor tRNAs. Nucleic Acids Res 22: 1327-1334.

55. Blanchet S, Cornu D, Hatin I, Grosjean H, Bertin P, et al. (2018) Deciphering the reading of the genetic code by near-cognate tRNA. Proc Natl Acad Sci U S A 115: 3018-3023.
56. Haas M, Vlcek V, Balabanov P, Salmonson T, Bakchine S, et al. (2015) European Medicines Agency review of ataluren for the treatment of ambulant patients aged 5 years and older with Duchenne muscular dystrophy resulting from a nonsense mutation in the dystrophin gene. Neuromuscul Disord 25: 5-13.
57. Hettig RA, Adcock JD (1946) Studies on the toxicity of streptomycin for man; a preliminary report. Science 103: 355-357.
58. Greenwood GJ (1959) Neomycin ototoxicity; report of a case. AMA Arch Otolaryngol 69: 390-397.
59. Moosajee M, Tracey-White D, Smart M, Weetall M, Torriano S, et al. (2016) Functional rescue of REP1 following treatment with PTC124 and novel derivative PTC-414 in human choroideremia fibroblasts and the nonsense-mediated zebrafish model. Hum Mol Genet 25: 3416-3431.
60. Rowe SM, Sloane P, Tang LP, Backer K, Mazur M, et al. (2011) Suppression of CFTR premature termination codons and rescue of CFTR protein and function by the synthetic aminoglycoside NB54. J Mol Med (Berl) 89: 1149-1161.
61. Wang D, Belakhov V, Kandasamy J, Baasov T, Li SC, et al. (2012) The designer aminoglycoside NB84 significantly reduces glycosaminoglycan accumulation associated with MPS I-H in the Idua-W392X mouse. Mol Genet Metab 105: 116-125.
62. Love MI, Huber W, Anders S (2014) Moderated estimation of fold change and dispersion for RNA-seq data with DESeq2. Genome Biol 15: 550.

Author contributions: CT, SA, CB, CL, VM, JMS, HB, TC, RG, DH, AM, GNY, MCC, PAM and FL performed experiments. SA, CB, VM, EDB, JMS, DT, YM, SR and FL wrote the manuscript. CT, SA, CB, EDB, JMS, EW, AP, PR, DH, MG, EA, MH, AK, EW, YM, SR and FL designed the experiments and analyzed the data.

.

Competing interests: Authors declare that they have no competing interest.

Data and material availability: Data and materials are fully available.

Figure Legends

Fig. 1. Identification of DAP as an efficient and exclusive corrector of UGA nonsense mutations. (**A**) Fractionation pathway of H7 *L. inversa* extract starting from fraction F87-1. (**B**) Schematic representation of the firefly luciferase construct used to measure readthrough activity. HeLa cells were transfected with an expression vector carrying a firefly luciferase (Fluc) gene consisting of the open reading frame encoding firefly luciferase interrupted by an intron and a nonsense codon at position 109. (**C**) Luciferase activity in HeLa cells transfected with the construct described in (B) carrying a UGA, UAA, or UAG PTC and incubated with DMSO, H7 extract, one of various H7 fractions, or DAP. the value of each luciferase measurement is presented on the table on the right side of the graph. (**D**) Readthrough activity on the construct described in (B) as a function of the G418 or DAP dose. Error bars represent SD. All data shown in Figures 1-C and -D are representative of two independent experiments.

Fig. 2. DAP restores the synthesis of the endogenous TP53 gene carrying a UGA nonsense mutation but not if it carries a UAA or UAG nonsense mutation. Calu-6 (top), Caov-3 (middle), and Caco-2 (bottom) cells were incubated with increasing amounts of DAP or G418 before purifying proteins and monitoring the level of p53 protein by western blotting. The molecular weight is indicated on the left side of each gel. Results are representative of two independent experiments.

Fig. 3. DAP restores the function of p53 in Calu-6 cells. (**A**) Schematic representation of the construct used to measure the function of p53. The construct carries a cDNA encoding the firefly luciferase under a promoter having two p53-responsive elements (underlined). The arrow indicates the transcription start. (**B**) Luciferase activity in Calu-6 cells transfected with the construct described in (A) and treated with DMSO, DAP, or G418. The luciferase activity depends on the amount of functional p53 protein. (**C**) Level of p21 mRNA measured by quantitative RT-PCR in Calu-6 cells treated with DMSO, DAP, or G418. The level of p21 mRNA is related to the amount of functional p53 protein synthesized in the cell. (**D**) DAP restores the function of CFTR in cystic fibrosis patient cells carrying a nonsense mutation on both CFTR alleles. Nose epithelial cells from three unrelated cystic fibrosis patients were incubated with the fluorescent molecule SPQ and with DMSO, G418 at 600µM, or DAP at 25µM before measuring the fluorescence, whose intensity correlates with the presence of functional CFTR at the cell membrane. The results presented in panels B and C are representative of at least two independent experiments. Error bar= S.D., p=Test-student.

Fig. 4. DAP is not an NMD inhibitor and is not toxic. (**A**) Ratio of the level of p53 mRNA to that of GAPDH mRNA, as measured by RT-PCR, in Calu-6 cells treated with DMSO, DAP, or G418. The ratio calculated for DMSO treatment is arbitrarily set at 1. (**B**) Adenylate kinase activity in the culture medium of HeLa cells treated with DMSO (0), increasing

amounts of DAP, or the apoptosis inductor staurosporine (STS). The results presented in Figure 4 are representative of two independent experiments. Error bar= S.D., p=Test-student.

Fig. 5. DAP corrects UGA nonsense mutations *in vivo*. (**A**) Chromatograms illustrating the stability of DAP after 4 hours of incubation in S9 mix (in duplicate, two upper panels) as compared to the amount of DAP extracted at T0 (in duplicate, two lower panels). (**B**) 28 nude mice were injected with Calu-6 or HCC-GR6 cells to promote tumor development. The mice were exposed to DMSO or DAP for about three weeks and tumor size was measured three times weekly and plotted on the graph. For each experimental condition, 7 mice were used. (**C**) Western blot analysis of p53 protein in the Calu-6-cell tumors of the seven DMSO-exposed and seven DAP-exposed mice. GAPDH was used as loading control. The results presented in Figure 5 are representative of two independent experiments. Error bar= S.D., p=Test-student.

Fig. 6. DAP interferes with the activity of FTSJ1. (**A**) Determination by mass spectrometry (MS/MS spectrum) of the amino acid incorporated at the PTC position. Firefly luciferase from HEK293FT cells transfected with the Fluc-int-UGA construct was immunoprecipitated and the identity of the amino acid incorporated at the PTC position was determined by mass spectrometry. The one-letter amino-acid sequence of Firefly luciferase is indicated on the top of the graph with the presence of the tryptophan (W) at the PTC position (**B**) *Left panel*: The efficiency of UGA readthrough by DAP decreases with increasing amounts of FTSJ1 but not with increasing amounts of CTU1. Readthrough efficiency was determined by measuring luciferase activity in HeLa cells co-transfected with the firefly luciferase construct described in Figure 1B and either with increasing amounts an expression vector for FTSJ1 or CTU10 (5, 1, or 2 µg). The empty expression vector (E.v.) was used as control. The cells were then exposed to 0, 0.39, 0.78, 1.56, 6.25, 25, 100, 300, or 600 µM DAP for 24 hours before measuring the luciferase activity. The experiment was performed twice and the results of both experiments (Exp1 and Exp2) are shown. *Right panel*: Western blot analysis of FTSJ1 and CTU1. (**C**) 2'-O-methylation analysis of tRNA^{Trp}, tRNA^{SER}, and tRNA^{GLN} by RiboMethSeq. A MethScore was attributed to each tRNA 2'-O-methylation for tRNA purified from HeLa cells treated with DAP (dark green histogram) or DMSO (light green histogram). The result of three independent experiments is indicated with the symbols ■●▶. (**D**) Analysis of DAP affinity column eluates shows that DAP interacts with FTSJ1. HeLa-cell extract was incubated with DAP covalently bound to beads or with beads alone. Proteins bound to the columns were eluted with excess DAP and the eluates analyzed by western blotting. Error bar= S.D., p=Test-student.

Table 1. Micronucleus induction assay. L5178Y TK$^{+/-}$ mouse lymphoma cells were exposed to increasing doses of DAP (as indicated), DMSO (DAP concentration 0 µM), or mitomycin or cyclophosphamide used as positive controls. 1000 cells were analyzed per condition and the number of micronucleated cells is reported. The experiment was performed in the absence (above) or presence (below) of S9 mix.

Table 2. Impact of DAP on the HeLa-cell transcription profile. The 20 genes showing more than four-fold overexpression (upper table) and the 10 genes showing more than four-fold down-regulation (lower table) in the presence of DAP are listed. Gene names, gene identifications (gene ID), log2fold changes, and p-values are indicated. Some information about the function of the gene is added in the last column.

Supplementary Materials

Materials and Methods

Transcriptomic analysis

Ten million HeLa cells were exposed to DMSO or DAP for 24 h. Total RNA was extracted with RNazol reagent. Libraries were prepared by poly(A) enrichment with a PolyA Spin mRNA Isolation Kit (Biolabs) and strand-specific cDNA libraries were prepared with the Illumina Truseq Stranded mRNA Sample Preparation Kit (Illumina Inc., USA). Reads were sequenced on an Illumina HiSeq 2500 device which produced six libraries of paired-end 100-nt long reads for three biological replicates of the two conditions. Reads were mapped with BWA-MEM (version 0.7.12-r1039, http://bio-bwa.sourceforge.net/) against the human genome (GRCh37.p13). Reads having passed the default Illumina filter procedure (chastity filter) were counted on human genes with featureCounts (version 1.5.1, http://subread.sourceforge.net/). Condition clustering was checked by principal component analysis with R package FactoMineR (version 1.36). Differential expression analysis was performed on the raw read counts with R package DESeq2 (version 1.14.1) [62]. Differentially expressed genes were determined with an adjusted p-value >0.05 and a |log2FC| >2. Heatmap representation of global gene expression of each library have

been produced using the normalized read counts (varianceStabilizingTransformation function of DESeq2) with R function heatmap.2 from R package gplots (version 3.0.1).

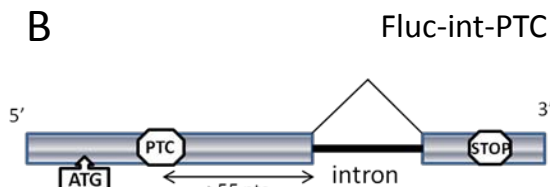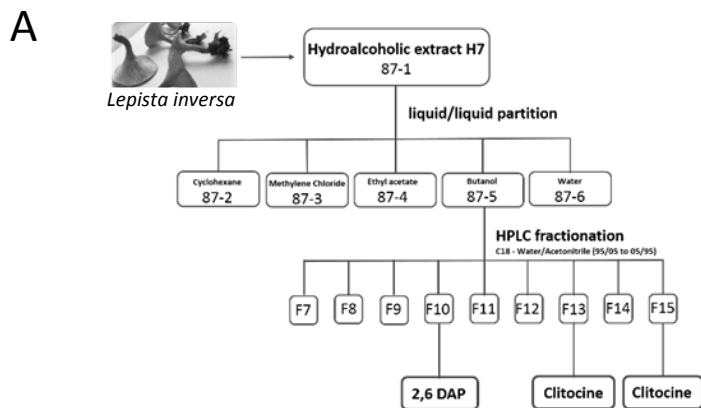*Two-dimensional differential gel electrophoresis*

2D-DIGE was performed on a mixture of protein samples labeled according to the CyDye minimal labeling method (GE Healthcare). Control, H7, and DA extracts were respectively labeled respectively with Cy2, Cy3, and Cy5 and pooled. Finally, 5.4 µL Destreak Reagent (GE Healthcare), 1% (v/v) IPG buffer pH 3 − 11NL (GE Healthcare) and CHAPS lysis buffer were added to reach a final volume of 450 µl. Migration in the first dimension, i.e. isoelectric focusing (IEF), was carried out with IPG strips pH 3 − 11NL, 18 cm (GE Healthcare), after overnight passive rehydration. IEF was carried out on an Ettan IPGphor 3 IEF unit (GE Healthcare) with the following parameters: (1) constant voltage of 150 V for 3 h, (2) constant voltage of 300 V for 3 h, (3) gradient from 300 V to 1000 V for 6 h, (4) gradient from 1000 V to 10000 V for 1 h, and (5) constant voltage of 10000 V for 2 h. The temperature was set at 20°C and the current was limited to 50 µA/strip. After the first dimension, the strips were equilibrated for 15 min in equilibration buffer containing 50 mM Tris-HCl pH 8.8, 6 M urea, 30% (v/v) glycerol, 2% (w/v) SDS, 0.02% Bromophenol Blue supplemented with 1% (w/v) DTT and subsequently for 15 min in equilibration buffer supplemented with 2.5% (w/v) iodoacetamide. The strips were rinsed in cathode buffer, placed on top of the second-dimension gel, and sealed with low-melt agarose. Cathode and anode buffers were added in the electrophoresis tank (Ettan DALT six, GE Healthcare) and the gels were run at 20°C. The migration settings were: (1) 5 mA for 2 h and (2) 25 mA until the sample reached the end of the gel. Gels were scanned with a Typhoon FLA 9500 (GE Healthcare).

Figure Legends

Fig. S1. DAP does not interfere with the global cell transcription profile. (A) Heatmap representation of up- and down-regulated genes to show a low effect of the DAP on HeLa cells from three independent experiments. 3228 shown genes (adjusted p-value < 0,05) are represented by the normalized read counts with a log2 scale (see Supplementary Material). Dendrograms show the separation of control (DMSO1-3) VS DAP (DAP 1-3) treated libraries without clear pattern of dysregulation between samples. (B) Raw data for the transcriptomic analysis performed in triplicate on HeLa cells exposed to DMSO or DAP.

Fig. S2. 2D-DIGE analysis. Extracts of HeLa cells exposed to DMSO (T) or DAP (DAP) were loaded for 2D-DIGE. Cy2 was used to detect proteins from cells exposed to DMSO and Cy5 was used to detect proteins from cells exposed to DAP.

Fig. S3. Influence of DAP on tRNA modifications: 2'-O-methylation analysis of tRNAs by RiboMethSeq. A MethScore was attributed to each tRNA 2'-O-methylation in tRNA purified from HeLa cells treated with DAP (dark green histogram) or DMSO (light green histogram).

A

Lepista inversa

Hydroalcoholic extract H7
87-1

liquid/liquid partition

| Cyclohexane 87-2 | Methylene Chloride 87-3 | Ethyl acetate 87-4 | Butanol 87-5 | Water 87-6 |

HPLC fractionation
C18 - Water/Acetonitrile (95/05 to 05/95)

F7 F8 F9 F10 F11 F12 F13 F14 F15

2,6 DAP   Clitocine   Clitocine

B

Fluc-int-PTC

5'   ATG   PTC   >55 nts   intron   STOP   3'

C

Luciferase activity (arbitrary units)
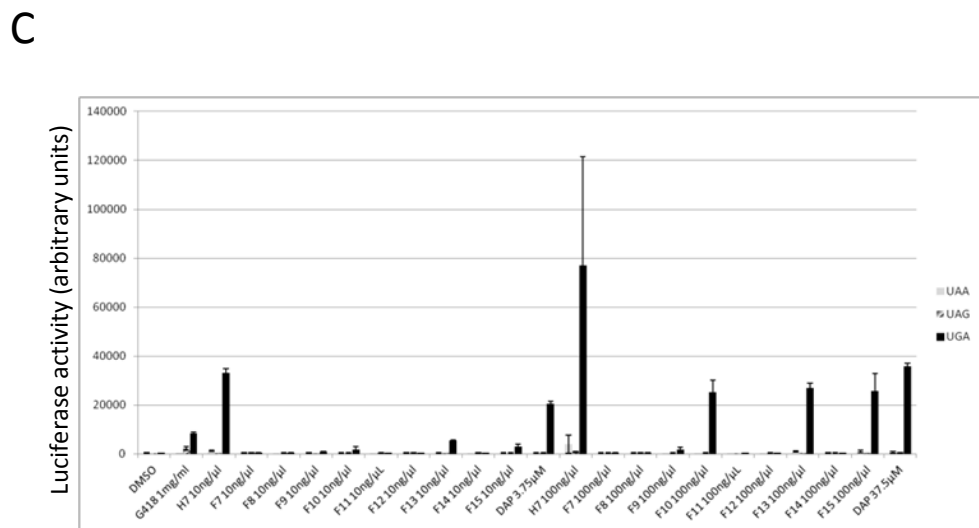
	UAA	UAG	UGA
DMSO	373±59	364.5±9	458.25±19
G418 1mg/m	495±34	2275.5±805	8466.25±478
H7 10ng/µl	1282.75±259	508.25±22	33049.25±1771
F7 10ng/µl	384.25±55	416.75±9	440.75±49
F8 10ng/µl	370.75±31	394.75±40	442.75±40
F9 10ng/µl	370.5±68	386±3	796.5±324
F10 10ng/µl	456±89	392.75±5	1865.25±1120
F11 10ng/µL	338±28	414.25±55	447±16
F12 10ng/µl	353.5±86	379.5±37	552±89
F13 10ng/µl	462.5±98	449.5±18	5567.25±148
F14 10ng/µl	327±68	410±105	495.25±22
F15 10ng/µl	403.5±28	386±40	2908±1039
DAP 3.75µM	370.75±86	366.5±43	20599.75±1015
H7 100ng/µl	3920±3712	807±321	76940.5±44413
F7 100ng/µl	355.75±83	405.75±55	443±83
F8 100ng/µl	368.75±58	390.5±34	386.25±71
F9 10ng/µl	351±40	384±61	1874±873
F10 100ng/µl	355.5±40	388±43	25119.75±4908
F11 100ng/µl	329.75±65	386±16	464.75±28
F12 100ng/µl	357.5±37	388.25±37	488.75±37
F13 100ng/µl	1106.25±225	493±80	26916±2085
F14 100ng/µl	362±49	405.75±37	565±52
F15 100ng/µl	999±419	492.75±49	25660.75±7203
DAP 37.5µM	610.75±408	451.5±145	35939.75±1176

D

Luciferase activity (arbitrary units)

DMSO   0,39µM   0,78µM   1,56µM   6,25µM   25µM   100µM   300µM   600µM

DAP
G418

Figure 1

Figure 2

A

P53 response
elements

AGACATGCCTAGACATGCCTAACCGGTTAGACATGCCTAGACATGCCT
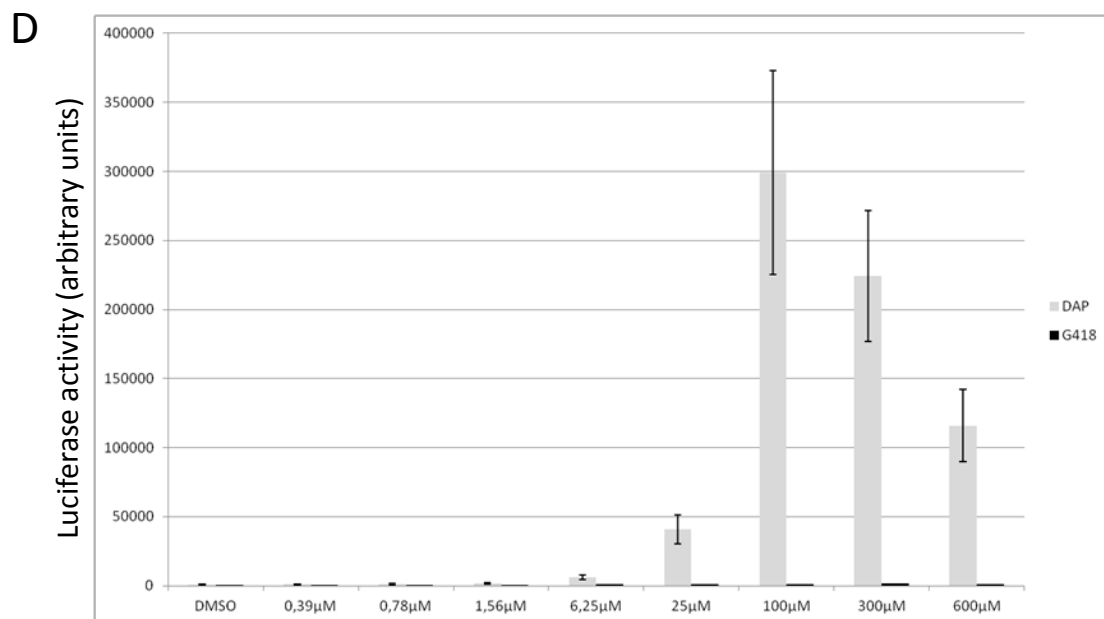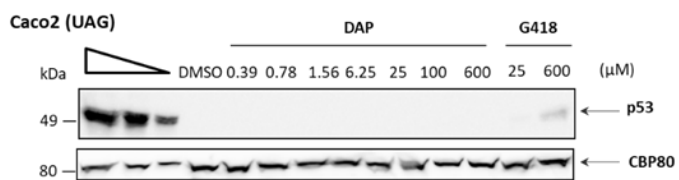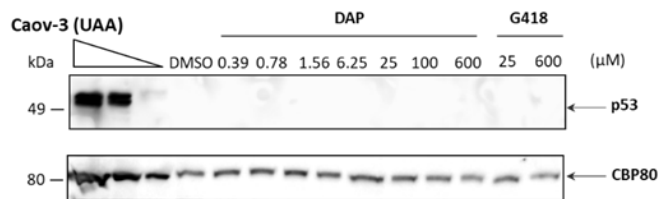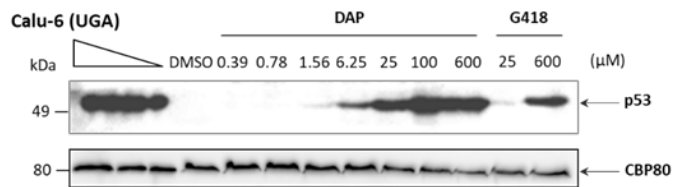
Fluc cDNA
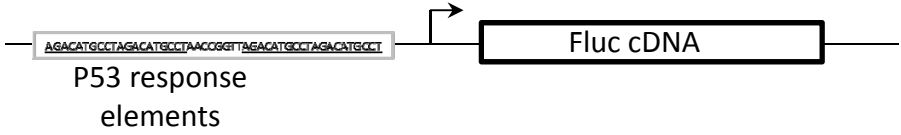
B
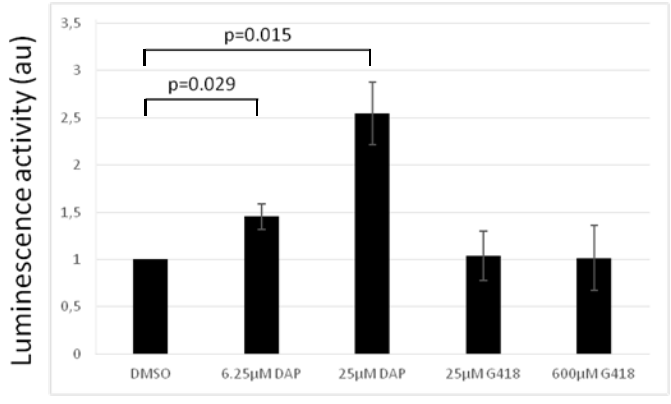
C
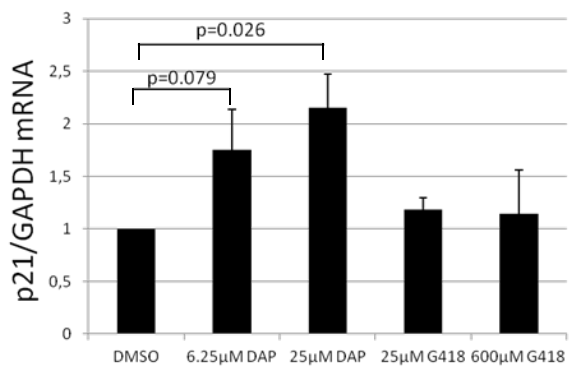
D
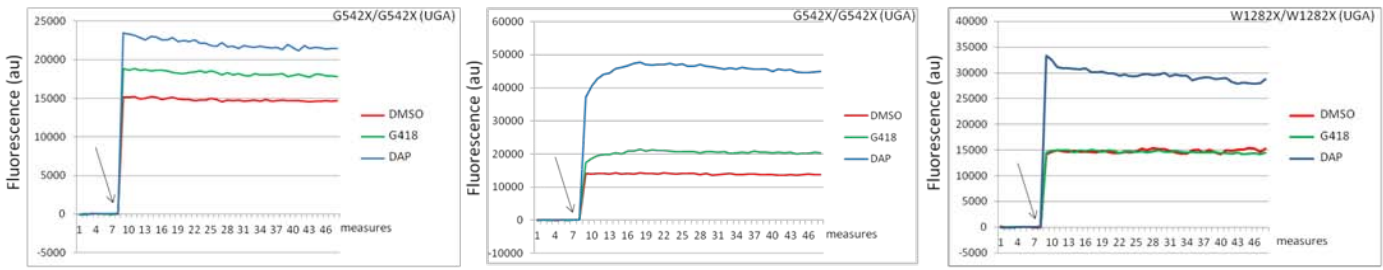
Figure 3

A
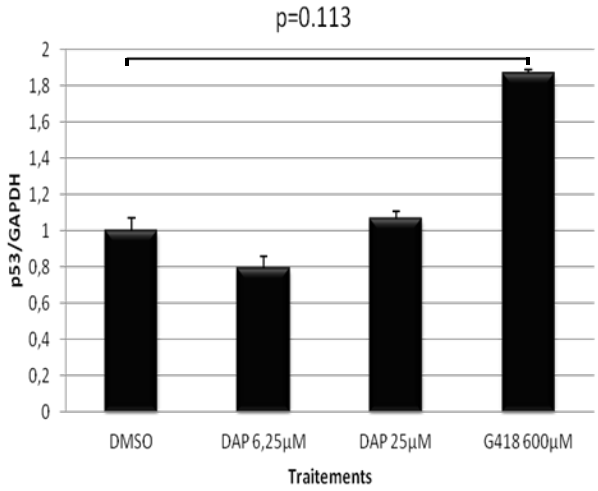
B
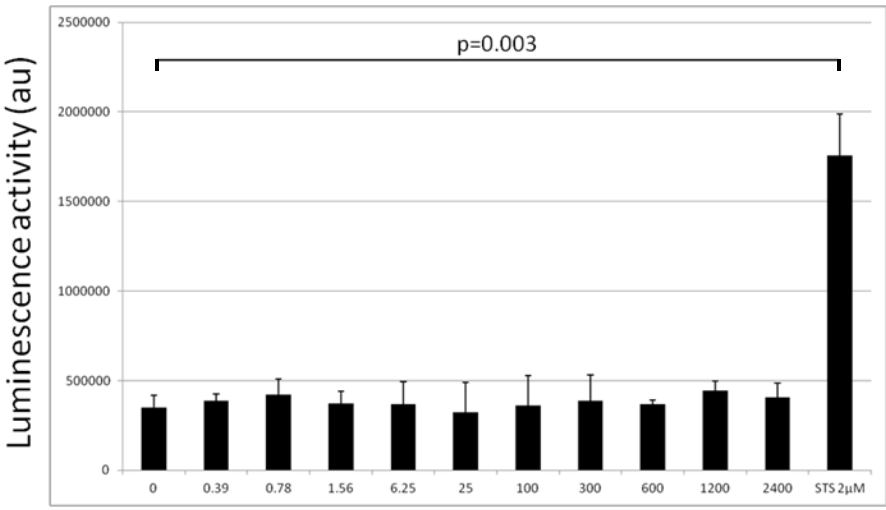
Figure 4

A DAP

B

Calu-6

HCC-GR6

DMSO
DAP

Tumor volume (cm³)

p=0.002 p=0.011 p=0.003 p=0.001 p=0.002 p=0.002 p=0.014 p=0.011 p=0.006 p=0.009 p=0.012 p=0.015 p=0.013 p=0.017 p=0.007

measures
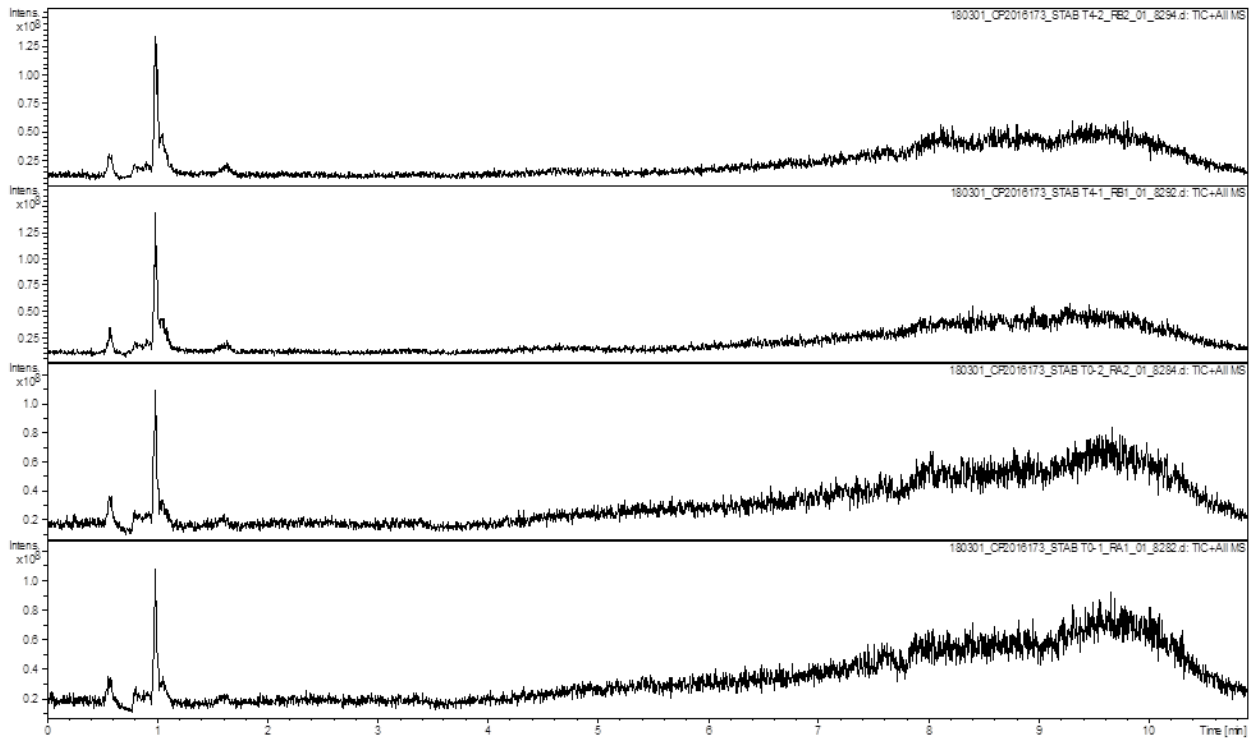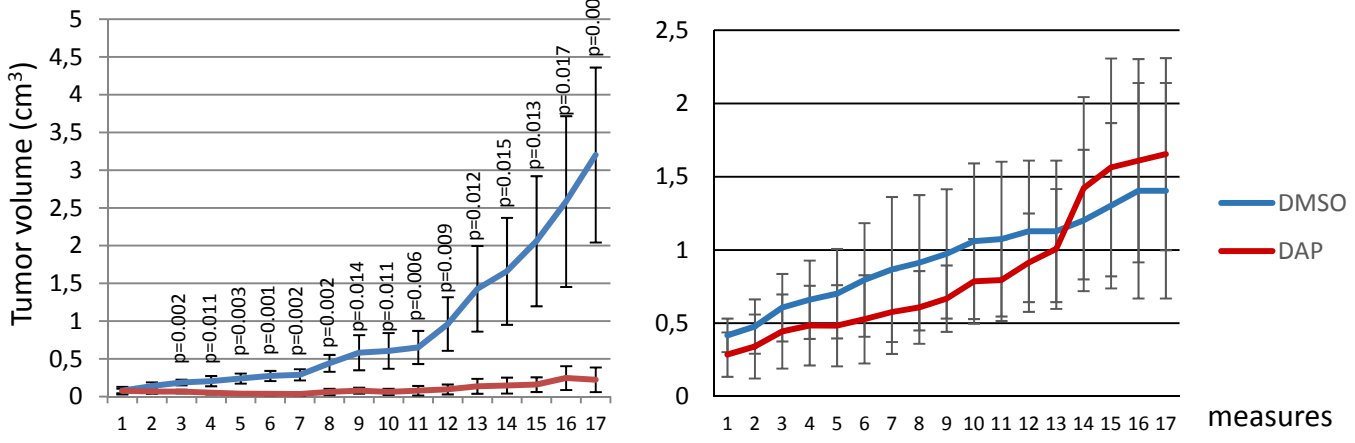
C

DMSO   DAP   HCC-GR6   treatment

← p53

← GAPDH
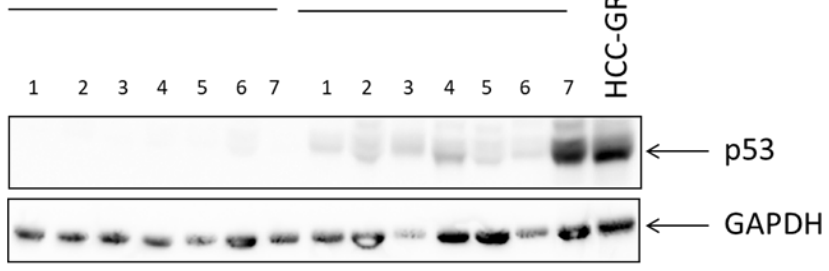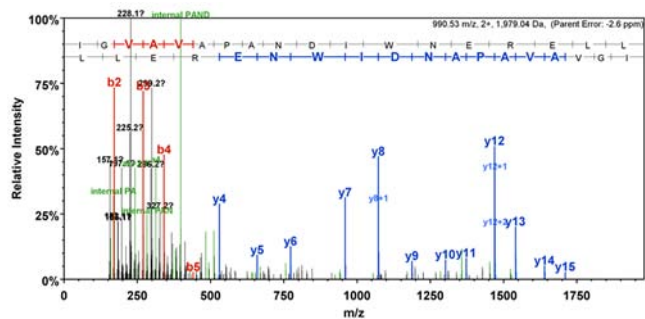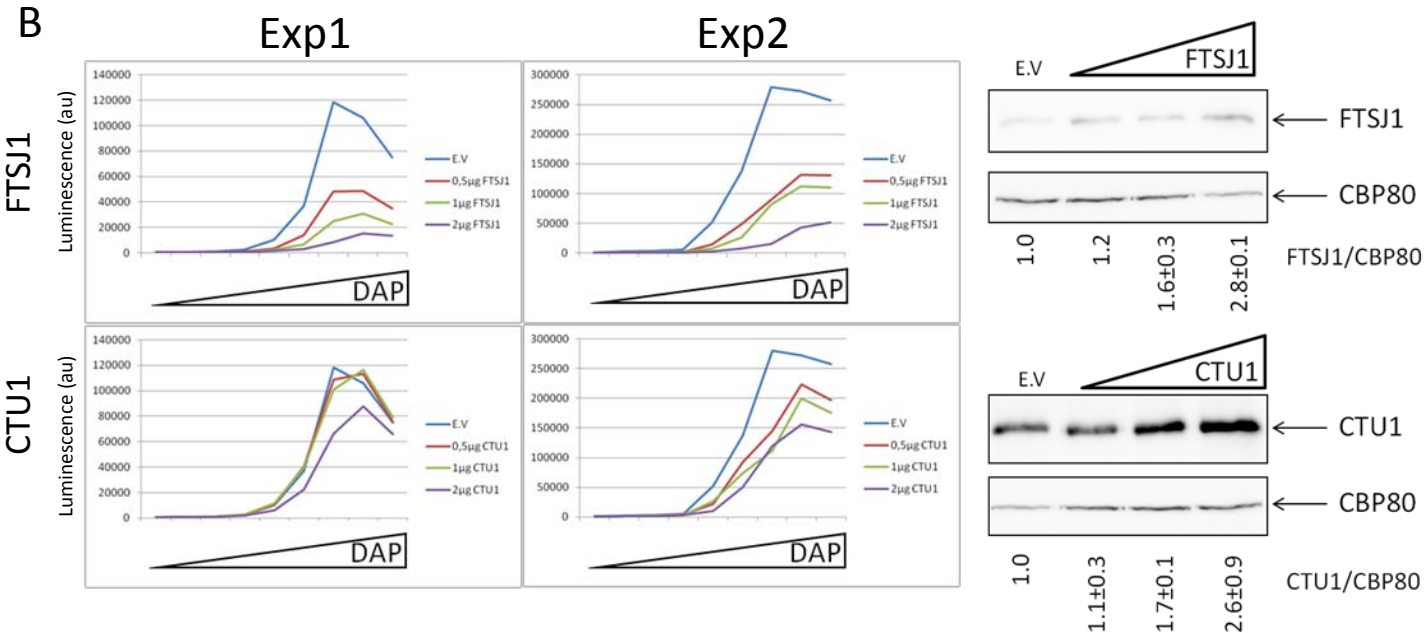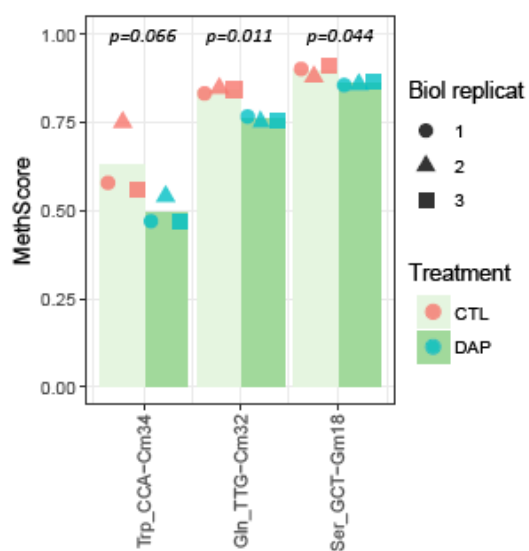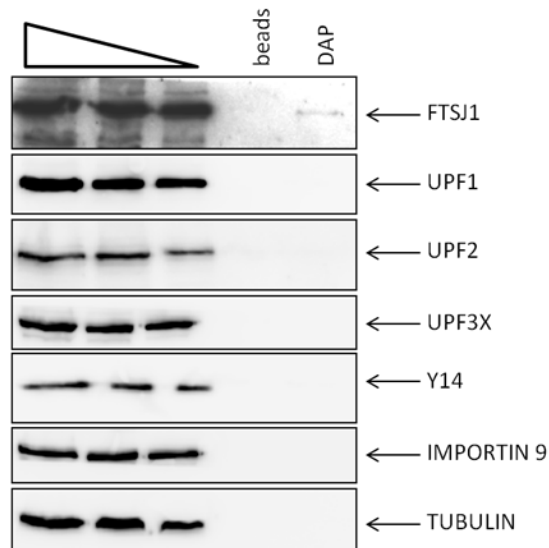
Figure 5

Figure 6

| Treatment conditions	DAP dose (µM)	Micronucleated cells
Assay without S9 mix	0	0
	20	2
	40	3
	70	1
	Mitomycin (1 µg/ml)	100
Assay with S9 mix	0	0
	40	0
	290	1
	580	0
	Cyclophosphamide (6 µg/ml)	60

Table 1

List of the 20 genes showing at least 4-fold upregulation in the presence of DAP

Gene Name	GeneID	log2FoldChange	p-value	Gene function
S100A5	6276	6.119	3.080E-68	S100 family member involved in Ca2+ intracellular regulation
CMYA5	202333	3.442	1.899E-33	Anchor protein of PKA
DCHS1	8642	3.427	9.008E-18	Cadherin family member
LRIT3	345193	3.040	1.221E-13	Immunoglobulin-like protein
STC2	8614	2.836	7.358E-64	Secreted protein putatively involved in Ca and phosphate transport
GRK7	131890	2.771	4.546E-12	Retina-specific kinase
IL18BP	10068	2.635	2.408E-12	inhibitor of the proinflammatory cytokine IL18
ITGA10	8515	2.458	2.317E-09	integrin involved in cell adhesion
ACRC	93953	2.441	1.663E-19	putative nuclear protein
TRIB3	57761	2.430	1.419E-28	putative protein kinase induced by the transcription factor NF-kappaB
ASNS	440	2.217	5.830E-79	Asparagine synthetase
ZNF721	170960	2.216	1.117E-26	putative transcriptional regulator
PNLDC1	154197	2.206	6.267E-11	PARN Like, Ribonuclease Domain Containing 1
NUP210L	91181	2.200	8.162E-08	nucleoporin 210 like
ZNF460	10794	2.196	5.326E-10	Zinc finger protein
ANKRD11	29123	2.186	4.476E-58	protein interacting with histone deacetylases
SPEN	23013	2.164	2.006E-92	hormone inducible transcriptional repressor
SESN2	83667	2.158	2.522E-19	member of the sestrin family of PA26-related proteins
CNTF	1270	2.096	1.291E-07	neurotrophic factor
ADAM32	203102	2.049	4.829E-07	member of the disintegrin family

List of the 10 genes showing at least 4-fold downregulation in the presence of DAP

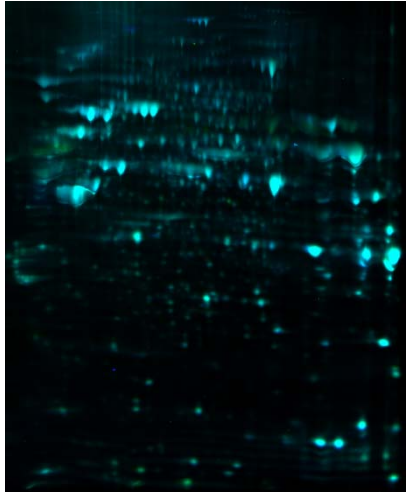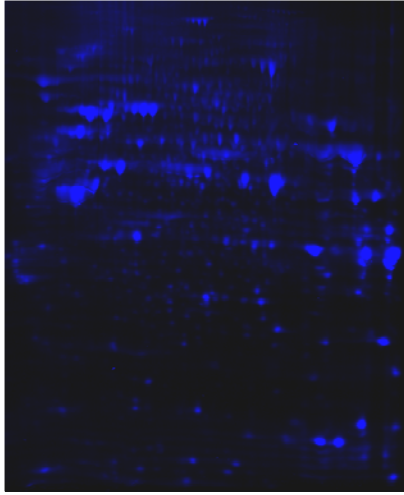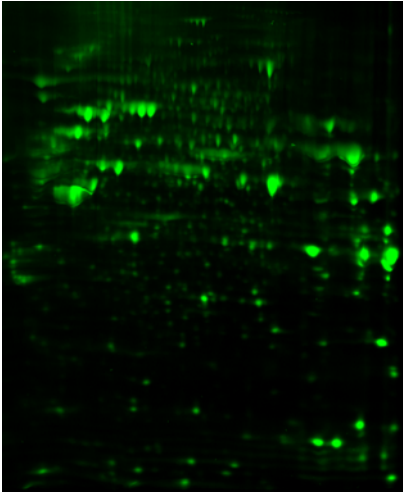| Gene Name	GeneID	log2FoldChange	p-value	Gene function
COX2	4513	-3.516	1.361E-102	protein involved in the synthesis of prostaglandins
COX3	4514	-3.286	4.176E-86	COX-3 is an enzyme encoded by the PTGS1 gene
ND6	4541	-2.779	2.717E-36	This protein is not functional in humans
COX1	4512	-2.516	2.860E-36	subunit of the respiratory chain Complex I
SYNC	81493	-2.233	3.857E-10	Cytochrome c oxidase subunit I
HSD17B8	7923	-2.144	4.807E-10	member of the intermediate filament family
ATP8	4509	-2.113	5.218E-19	Estradiol 17 beta-dehydrogenase 8
OLR1	4973	-2.065	1.925E-30	mitochondrial ATP synthase Fo subunit 8
INSL4	3641	-2.029	9.034E-21	Oxidized low-density lipoprotein receptor 1
IDH2	3418	-2.015	4.480E-09	insulin-like 4 protein Isocitrate dehydrogenase

Table 2

A
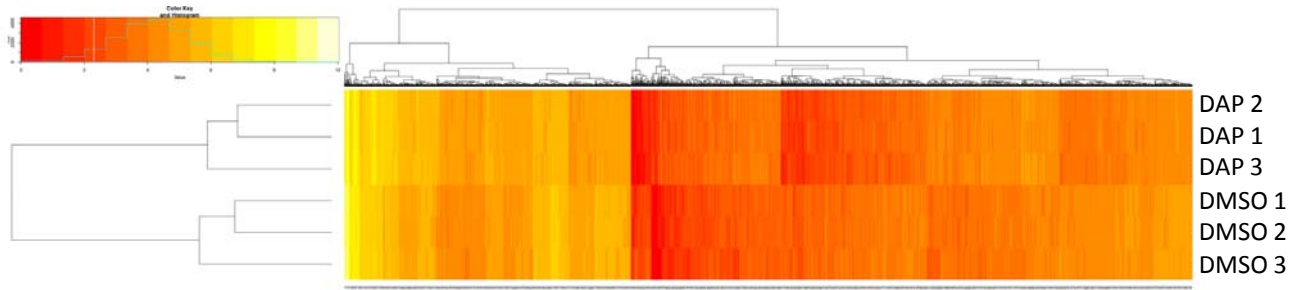
B

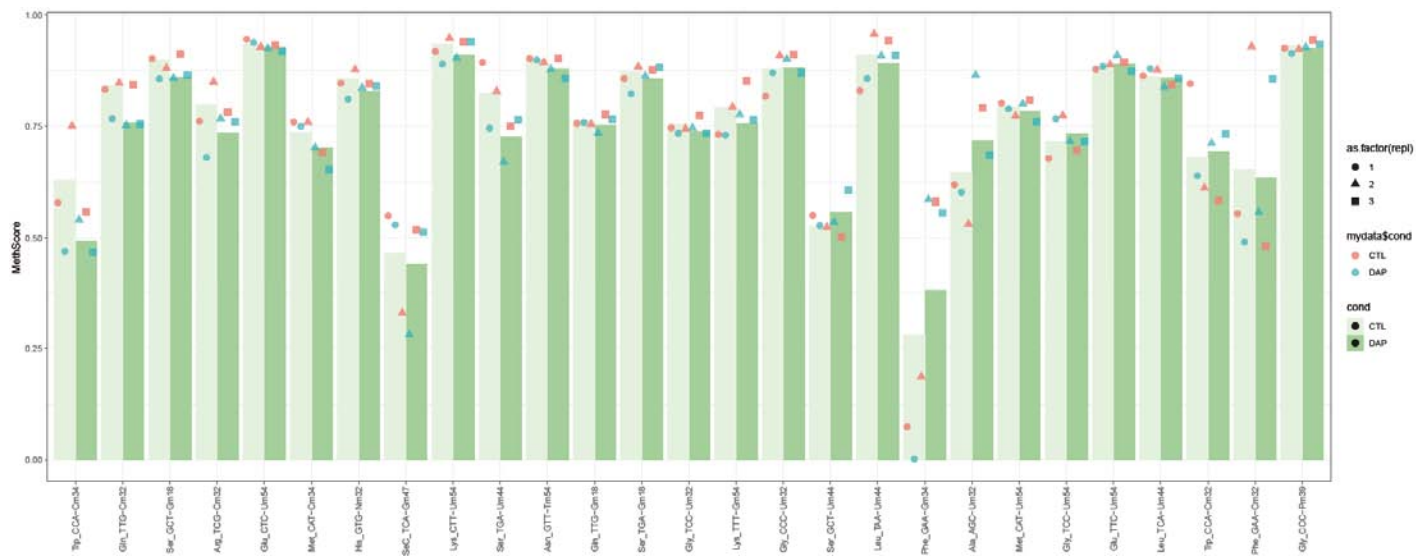see attached file for Raw data

Cy2 : T-   Cy5 : DAP   Merge

Supplemental Figure S2

Supplemental Figure S3